Beni-Suef University Journal of Basic and Applied Sciences

RESEARCH

Open Access

Numerical simulation of a diesel engine performance powered by soybean biodiesel and diesel fuels

Mohamed Khaled Abdelrazek*, Mohsen Mohamed Abdelaal and Ahmed Mustafa El-Nahas

Abstract

Background The present study presents a 3-D numerical simulation of a direct injection diesel engine powered by base diesel oil and soybean biodiesel fuel at different load conditions. The modeling was performed using commercial computational fluid dynamics (CFD) software linked to a chemical solver. A chemical kinetic reaction mechanism was developed to simulate the combustion and fuel spray processes. Base diesel oil results were verified using a single-cylinder, 4-stroke diesel engine.

Results The study showed that the usage of the soybean biodiesel fuel caused a reduction in carbon monoxide (CO) and hydrocarbon (HC) emissions by about 42.38% and 41.35%, compared with base diesel and an increase in nitrogen oxides (NO_x) and carbon dioxide (CO_2) emissions of about 21.8% and 11.2%, respectively. Exhaust gas temperature (EGT) is reduced by an average value of 9.4%, the brake-specific fuel consumption (BSFC) is increased by an average value of 11.8% and the brake thermal efficiency (BTE) is dropped by an average value of 11.3% for soybean biodiesel fuel.

Conclusions The CFD model showed the effect of the unsaturated fatty acid methyl esters present in soybean biodiesel on the spatial distributed values of NO_x, oxygen and temperature during the combustion in engine cylinder. It was observed that the combustion of soybean biodiesel began about 3.89 CAD earlier than base diesel, and the in-cylinder peak pressure was dropped by 8.25%. Soybean biodiesel fuel was optimized by performing four starts of injection (SOI) at timings of − 18, − 16, − 15 and − 13,5 bTDC, and it was found that the combustion characteristics of soybean biodiesel are optimum at SOI = − 15 bTDC. These results indicate that the biodiesel fuel can be used as an alternative and environmentally friendly fuel in the engine without any modifications.

Keywords Biodiesel, Diesel engine, Combustion, Emission, Numerical simulation

1 Background

The increasing demand for fossil fuels and the concerns about their harmful emissions have forced the scientific society to search for alternative fuels for internal combustion engines. Therefore, researchers have been developing new alternatives from different sources, biodiesel fuel is one of the best alternative fuels for diesel engines because of its high cetane number, low carbon fuel, non-toxic, biodegradable, lubricity, oxygenation nature, no aromatics and almost no sulfur content, so it is considered a renewable energy source and environmentally friendly [1–4].

Vegetable oils, animal fats and reused oils are the most common sources of biodiesel. Biodiesel fuel is produced by a common chemical method, namely transesterification; in this method, a chemical reaction occurs between the triglycerides (vegetable oil) and alcohol in

*Correspondence:
Mohamed Khaled Abdelrazek
eng.mohammadkh94@gmail.com
Department of Mechanical Engineering, Faculty of Engineering, Al–Azhar University, Cairo 11371, Egypt

the presence of a catalyst. If methanol alcohol is used, the reaction products will be fatty acid methyl esters (FAMEs; biodiesel) and glycerol. FAMEs may be saturated and unsaturated; their proportions in biodiesel fuel directly affect the physical and chemical properties [5–7].

Soybean biodiesel fuel is considered in the present study. However, the disadvantages of soybean biodiesel relative to base diesel oil, such as higher viscosity, higher density and lower volatility. So, the usage of biodiesel for a long term may cause engine durability problems such as poor fuel atomization, injector coking, piston ring sticking, a clogged fuel filter and higher pressure inside fuel lines [8]. Therefore, different experimental methods are required to make soybean biodiesel more suitable for diesel engines such as preheating at a wide range of temperatures, blending with base diesel, increasing injection pressure and adding additives [9]. CFD codes have recently gained popularity in the industry as a tool for facilitating and speeding up engine evaluation under various conditions. The purpose is to minimize the cost and prototyping time and have the ability to make several studies by changing individual parameters such as injection pressure, inflow temperature of the fuel and air, injection timing, fuel blends and the engine loads [10, 11].

A compression ignition (CI) engine is considered one of the most complex problems in fluid dynamics to model because the flow inside the cylinder is unsteady, compressible, turbulent and cyclic. All physical processes that take place inside the cylinder from the start of air entry to the end of combustion required a mathematical model to describe them. Turbulence, fuel spray, atomization, breakup, collision, coalescence, droplets vaporization, kinetic reaction mechanism (fuel chemistry), self-ignition, premixed and diffusion combustion, heat losses and emission development (NO_x and soot)—all of these processes require subroutines that work together in order to simulate the engine [12, 13].

Many studies conducted on biodiesel fuel and its effect on engine performance, Zhang et al. [14] studied the performance and emission of a marine diesel engine fueled with natural gas ignited by biodiesel blends at different conditions of engine load and concluded that at all engine conditions, the NO_x, CO and soot emissions decreased with increasing the natural gas fraction. According to EL-Seesy et al. [15], the addition of butanol to the diesel/jojoba oil blend lowers the mixture's viscosity compared to diesel/jojoba oil, increases the in-cylinder peak pressure and heat release rate (HRR), and also results in a reduction in NO_x, CO and HC emissions compared to diesel fuel. Zhang et al. [16] conducted a study on the effect of assisted hydrogen on a diesel engine performance fueled with biodiesel fuel and reported that the in-cylinder pressure and temperature are increased by about 7.42% and 7.14%, respectively. Meanwhile CO and HC decreased but NO_x emissions increased. Coughlin et al. [17] studied the combustion characteristics of soybean oil–butanol blends and found that the addition of alcohol could improve the soybean combustion characteristics. Ng HK et al. [18] studied the effect of palm, coconut and soybean biodiesel fuels on a diesel engine performance numerically using a CFD code, which was coupled to a chemical kinetic reaction mechanism including 80 species and 303 reactions. According this study, the biodiesel properties influence the formation of emissions; so, the soybean biodiesel fuel provided a greater thermal NO_x than others because its higher unsaturation level. Al-Dawody et al. [19] carried out a 2-D numerical and experimental study on a DI diesel engine fueled with different blends of soybean biodiesel with diesel fuels. The effects of blending on the in-cylinder pressure, heat release rate (HRR), unburned hydrocarbon (UHC), carbon monoxide (CO), nitrogen oxides (NO_x) and smoke opacity were calculated. He found that the use ofiesel results in lower smoke opacity up to 48.23% with higher brake-specific fuel consumption (BSFC) by 14.65%, compared to diesel fuel. For the blends of B20 (20% soybean biodiesel + 80% diesel fuel) and B100 (100% soybean biodiesel), the CO emissions reduced by 11.36% and 41.7% respectively, compared to diesel fuel. At blends of B20, B40 and B100, the unburnt hydrocarbon emissions were found to be 15%, 27% and 38.4% lower than that of diesel fuel, respectively. Also, he reported that at all blends the NOx emissions were observed to be higher than that of diesel fuel. The in-cylinder pressure for soybean biodiesel is lower than that of diesel fuel by about 2.98% due to the reduction in the heat supply for the blended fuel and the maximum pressure obtained for biodiesel is near to top dead center (TDC) than diesel fuel.

In contrast to conventional combustion, Ganesan et al. [20] investigated a light-duty diesel engine using the reactivity-controlled compression ignition technique by introducing cottonseed oil biodiesel as a high-reactivity fuel directly into the combustion chamber and n-pentanol as a low-reactivity fuel. In comparison with the neat cottonseed oil biodiesel, this method led to lower concentrations of NO_x and smoke emissions by roughly 44.2% and 35.0%, as well as a higher thermal efficiency. Nayak et al. [21] investigated the performance, combustion and emission characteristics of a direct injection diesel engine running on biodiesel fuel produced from waste palm cooking oil and fish oil and reported that the biodiesel fuel resulted in a lower thermal efficiency and higher specific fuel consumption compared to diesel fuel. An experimental study carried out by Singh et al. [22] on a diesel engine running on Jatropha biodiesel at

varied compression ratios. Jatropha biodiesel diesel blend (B30) and neat diesel fuel were used to power the diesel engine. According to the experimental study, using the B30 blend reduces HC and CO emissions from diesel by about 16.7% and 24%, respectively. However, using the B30 blend resulted in a notable increase in NO_x and CO_2 emissions. Gritsenko et al. [23] investigated how disconnecting some of the engine cylinders in low-load and idling modes increased fuel efficiency in cars and tractors. Experiment results indicate that when some engine cylinders are disconnected, the performance parameters of the car (tractor) are interdependent. It has also been established that the maximum reduction in hourly fuel consumption occurs when the engine is idling, and that it decreases as the load increases.

Due to its higher viscosity and lower calorific value, biodiesel causes CI engines to operate poorly and consume a lot of fuel. This issue can be solved by raising the injection temperature of biodiesel to a specific temperature. The results of an experimental study conducted by Kodate et al. [24] on a DI diesel engine running on preheated biodiesel fuel (at 95 °C) showed that the viscosity of the fuel decreases at higher temperatures, improving combustion characteristics and fuel atomization as well as fuel vaporization in a diesel engine, resulting in higher engine performance and lower CO and HC emissions with a slight increase in NO_x and CO_2 emissions when compared to unheated biodiesel fuel.

Biswas et al. [25] compared the performance, emissions and engine noise of a quadruple (early–pilot–main–after) injection strategy to three different triple [early–pilot–main and pilot–main–after] injection strategies in a heavy-duty BS-IV diesel engine with a 45% EGR fraction. According to this study, the quadruple injection strategy outperforms the promising triple injection strategy, which provides optimal results in terms of both performance and emissions. Using Fisher's primary breakup model, Beutler et al. [26] carried out numerical modeling on a spray of diesel and polyoxymethylene dimethyl ether in a high-pressure chamber at several variable parameters (ambient pressure, temperature and injection pressure) and compared it with the results of the experiments. Baek et al. [27] analyzed the spray behavior and the performance of a diesel engine powered by biodiesel and jet propellant-5 (JP-5) at multiple split injection strategies and reported that for all injection timings, biodiesel showed disadvantages as compared to JP-5 in terms of combustion and emission characteristics. Kuti et al. [28] used the Reynolds averaged Navier–Stokes model to simulate the spray combustion characteristics of waste bio-oils and traditional diesel fuel. They used a combination of *n*-heptane and *n*-tetradecane as surrogates for diesel fuel and a combination of methyl decanoate, methyl-9-decenoate and *n*-heptane as surrogates for the waste bio-oils. The results of the spray liquid length, ignition delay period, soot formation and flame lift-off length were compared to the experimental results, and good validity was found.

Although biodiesel derived from rice bran oil is seen to be a viable green fuel substitute for traditional diesel fuel, when utilized as fuel in diesel engines. Particularly in cold areas, the high free fatty acid concentration of rice bran biodiesel fuel is viewed as a significant disadvantage. More specifically, this undesirable characteristic causes noticeably higher viscosity, surface tension and higher density, which may then cause problems with fuel pumping, poor fuel spray and atomization, the formation of heterogeneous air–fuel mixtures and ultimately incomplete combustion [29]. The main factors causing wear, corrosion and abrasion in engines may be deposits created during the burning of biodiesel. In comparison with neat diesel, the use of biodiesel and plant oil-based fuels typically results in cylinder head carbon deposits, deposits on the injector tip and on the piston crown, degradation of lubricating oil and the formation of more deposits. This is especially true for long-term applications [30].

Fuel stability is a main procedural problem regarded in biodiesel manufacturing and is related to several issues like phase separation, polymerization, fuel degradation and oxidation. There are three types of biodiesel stability: oxidation, storage and thermal stability. When biodiesel is kept in storage for a long time, oxidation occurs. During the storage time, the free radicals attack the unsaturated lipids in biodiesel and produce lipid peroxide products. The oxidation of biodiesel fuel is brought on by the double and triple bonds that are present in the chains of fatty acid methyl esters. Some of the extrinsic elements that impact the oxidative stability of biodiesel include the presence of air, light, antioxidants, metal traces and storage container material [31].

Compared to the previous studies, the diesel engine simulation process saves the time and effort of practical experiments. It also enables us to conduct several parametric studies for engine development. From this perspective, this study was chosen to evaluate the performance of the diesel engine, where the numerical results of conventional diesel fuel were compared with the experimental results, and a good convergence was found. A suitable kinetic reaction mechanism was chosen to simulate soybean-derived biodiesel, and the combustion and emission results were compared with previous works, and good validity was attained. In order to accurately simulate the in-cylinder turbulence, fuel atomization, droplet vaporization, kinetic reaction mechanism, premixed and diffusion combustion, heat losses and exhaust emission generation, it is necessary for many

Table 1 Fatty acid methyl ester composition of soybean biodiesel

FAMEs	Relative percentage
Methyl palmitate $C_{17}H_{34}O_2$	9.4
Methyl stearate $C_{19}H_{38}O_2$	4.1
Methyl oleate $C_{19}H_{36}O_2$	22
Methyl linoleate $C_{19}H_{34}O_2$	55.3
Methyl linolenate $C_{19}H_{32}O_2$	8.9

subroutines to work together. The objective of the current work is to create a 3-D computational fluid dynamics (CFD) model to simulate the combustion and emissions of a direct injection (DI) diesel engine running on diesel and soybean biodiesel fuels at different load conditions.

2 Fuel properties

Table 1 shows the faty acid methyl ester (FAME) composition of soybean biodiesel. The properties of the tested fuels are given in Tables 2 and 3, according to the

Table 2 Properties of base diesel fuel

Specification	Units	Test method	EN 590 limits		Test results
			min	max	
Typical formula					C14.16H25.21
Average molecular weight	g/kmol				195.5
Lower heating value	MJ/kg				42.93
Density at 15 °C	kg/m^3	EN ISO 3675, EN ISO 12185	820	860	838
Flash point	°C	EN ISO 2719	55	–	64
Sulfur content	mg/kg	EN ISO 8754	–	7000	2117
Cetane index		EN ISO 4264	46	–	53.8
Kinematic Viscosity 40 °C	mm^2/s	EN ISO 3104	2	4.5	2.317
Ash content	wt%	EN ISO 6245	–	0.01	0.0063
Polycyclic aromatic hydrocarbons	wt%	EN ISO 12196	–	11	7

Table 3 Properties of soybean biodiesel fuel

Specification	Units	Test method	EN 14,214 limits		Test results
			min	max	
Typical formula					C18.74H34.51O2
Average molecular weight	g/kmol				291.2
Lower heating value	MJ/kg				37.4
Density at 15 °C	kg/m^3	EN ISO 12185	–	900	883.4
Flash point	°C	EN ISO 3679	120	–	123
Sulfur content	mg/kg	EN ISO 20884	–	10	1.3
Cetane index		EN ISO 5165	51	–	54.1
Kinematic Viscosity 40 °C	mm^2/s	EN ISO 3104	3.5	5	4.512
Cold filter plugging point	°C	EN 116	–	+ 5 °C (summer) − 15° C (winter)	− 18
Water content	mg/kg	EN ISO 12937	–	500	357
Oxidation stability at 110 °C	hours	EN 14,112	6	–	7.1
Acid value	mg KOH/g	EN 14,104	–	0.5	0.36
Iodine value	g Iodine/100 g	EN 14,111	–	120	115
Methanol content	wt%	EN 14,110	–	0.2	0.11
Free glycerin	wt%	EN 14,111	–	0.02	0.01
Monoglyceride content	wt%	EN 14,105	–	0.8	0.5
Diglyceride content	wt%	EN 14,105	2	0.2	0.12
Triglyceride content	wt%	EN 14,105	–	0.2	0.16

European Union EN 590 and EN 14,214 standards. Due to the difference in physical and chemical properties of biodiesel fuel, the combustion and emission characteristics will be changed. The oxygen concentration in soybean biodiesel fuel is about 10.7 wt% [32]. This percentage of oxygen will directly influence on combustion and emission development, especially NO_x emissions. Also, properties such as cetane number will influence on the ignition delay period, as will viscosity, which is considered one of the most important parameters affecting the fuel spray, atomization and vaporization. Higher viscosity results in lower injection velocity, poor atomization, an increase in friction between the fuel boundary layer and fuel line surfaces, higher deposits and an increase in the power required for the fuel pump [33]. Soybean biodiesel fuel has a higher flash point than diesel fuel, which makes soybean biodiesel fuel safer during transporting and storing. The lower heating value of soybean biodiesel fuel is less than that of diesel fuel, thus HRR and BSFC may be decreased. Soybean biodiesel fuel has a chemical property known as an "acid number," which does not exist in diesel fuel properties. Acid number refers to the amount of free fatty acids (FFA) content in a fuel. FFA may be saturated or non-saturated, but its proportion will have a significant impact on the engine performance. Compared to diesel fuel, soybean biodiesel fuel is almost free from sulfur content, which is the main motives for using biodiesel fuel as an alternative fuel [34].

3 Experimental methodology

The present work has been conducted on a Petter PH1W single-cylinder, 4-stroke, naturally aspirated and water-cooled diesel engine with a hemispherical bowl in combustion chamber. The schematic diagram of the engine test bench is shown in Fig. 1. The engine specifications are tabulated in Table 4. A DC universal dynamometer is coupled to the diesel engine, which drives the engine at the start of operation and further absorbs the output power from the engine. A damping chamber with an orifice system is used to measure the inlet air mass flow rate supplied to the diesel engine and eliminate the pulsation effect at the engine suction. A piezoelectric sensor is used to measure the dynamic pressure inside the engine combustion chamber. A crankshaft position sensor is used

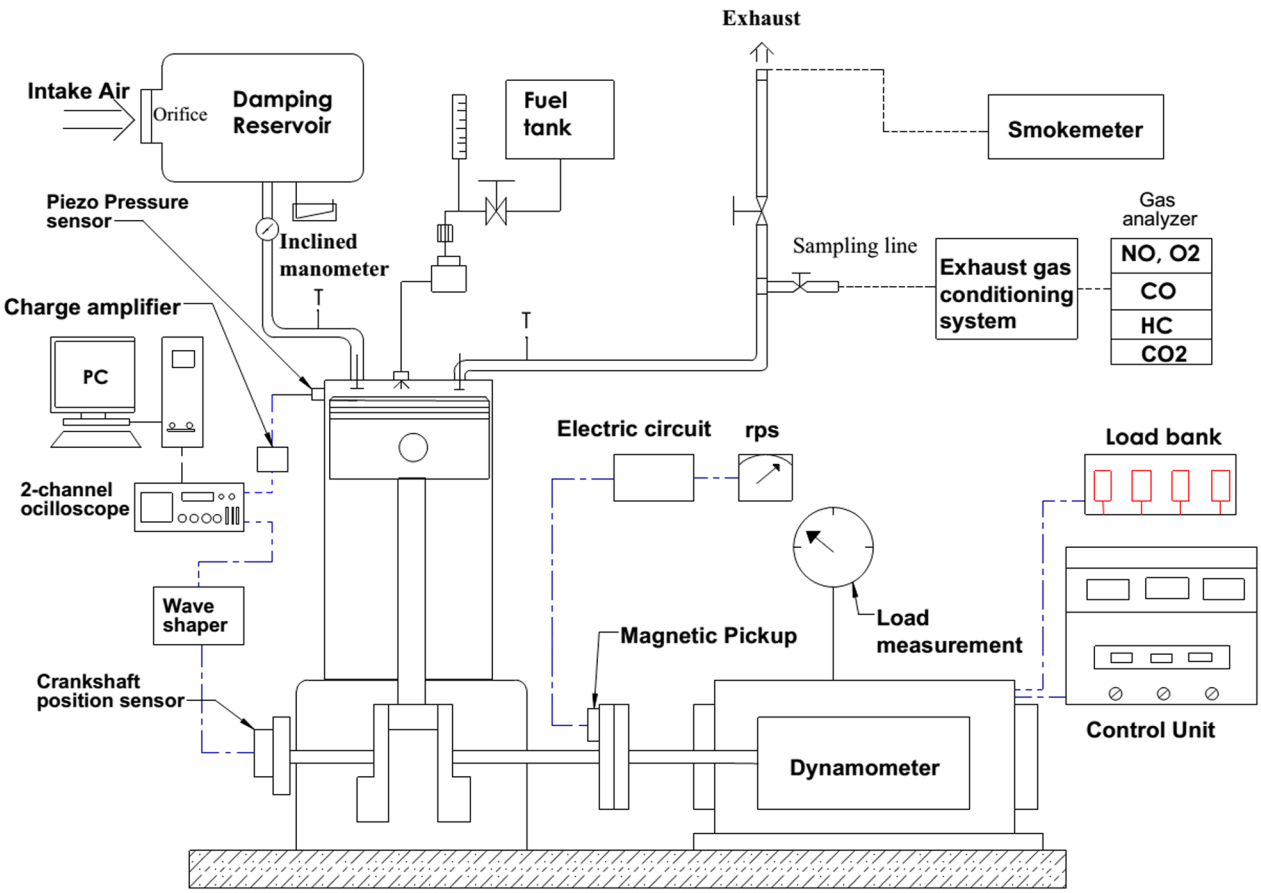

Fig. 1 Schematic diagram of the engine test bench

Table 4 Engine specifications

Engine model	Petter PH1W
Engine type	4-stroke, water-cooled diesel, naturally aspirated
No. of cylinder	1
Bore x stroke (mm)	87.3 X 110
Speed (rpm)	1500
Displacement (cm^3)	659
Compression ratio	16.5:1
Start of injection	− 20° bTDC
Injection duration (angles)	18°
Rated power (kw)	5.07 kw at 1500 rpm
Max. torque (Nm)	25 Nm at 1500 rpm

Table 5 Accuracy and relative error of measured parameters

Measured parameter	Accuracy	Relative error (%)
Engine brake power		3.96
Torque	±2%	2
Speed	±2%	2
In-cylinder pressure		4.92
Piezoelectric pressure sensor	±2%	2
Charge amplifier	±1%	1
Digitizing oscilloscope	±2%	2
Air flow rate	±0.2 mm H2O	1.64
Diesel fuel flow rate	$\pm 8.27 \times 10^{-3}$ kg/h	1.51
Thermocouple	±0.55 °C	1.57
Crankshaft position		3.9
Magnetic pickup	±1%	1
Wave shaper	±1%	1
NO	±5 ppm	5.88
CO	±1%	3.28
CO_2	±1%	3.57
HC	±3 ppm	3.08

to indicate the TDC position and the further intervals of crankshaft position. A 2-channel storage oscilloscope is used to present and record the in-cylinder pressure versus the crank angles. The exhaust gas temperature (EGT) is measured using a type K thermocouple with a sensitivity of 41 μV/°C and a standards error of ± 2.2 °C. The concentrations of CO, CO2, NO and HC emissions are measured using an ADC multi-gas analyzer. The tests have been conducted at a constant speed of 1500 rpm for a wide range of diesel engine load, starting from 20 up to 100% of the engine rated load. The characteristics of the equipment used are given in Table 5.

4 Numerical method

In the present study, numerical simulation is analyzed from intake valve closure (IVC) to exhaust valve opening (EVO); this simulation technique is known as closed cycle simulation (CCS). Due to the periodicity of the injector and the combustion chamber, the computational domain is divided into sectors in order to reduce the computational time. One eighth sector was taken to represent the full geometry. Piston bowl geometry, computational sector, sector mesh and the setting of nozzle orientation with the piston sliding motion inside the engine cylinder are shown in Fig. 2. Hexahedron mesh is generated through a commercial CFD code with a cell height of 1.6 mm, a cell expansion ratio of 1.01 from the piston and a cell expansion ratio of 1.01 from the head. Meshing can be automatically refined or coarsened based on the solution variables or geometrical features. Sub-processes such as a nozzle flow model, spray atomization, droplet breakup, droplet collision and coalescence, droplet vaporization and wall impingement have been needed to simulate the dynamics and interactions of the fuel spray. The nozzle orientation was adjusted according to the spherical coordinate system as $\theta = 134^{o}$ and $\phi = 22.5^{\circ}$. For fuel details, a combination of methyl decanoate (MD), methyl-9-decanoate (MD9D) and n-heptane is utilized as a reaction mechanism to represent the saturated and non-saturated of the oxygenated hydrocarbon chain of biodiesel fuel, which includes 247 species and 1129 reactions [35]. N-heptane reaction mechanism with 117 species and 472 reactions by [36] was utilized as a surrogate fuel model to represent the chemical kinetics of the diesel fuel. The model used for NO_x formation is based on thermal mechanism [37]. Fuel spray atomization and droplet breakup are modeled based on the Kelvin–Helmholtz / Rayleigh–Taylor (KH / RT) hybrid model, where the fuel spray is divided into two regions, the first region starting from the nozzle exit, during which the fuel jet still dense but some droplets are separated from the jet; this region is associated with Kelvin–Helmholtz modeling; see Fig. 3. At the end of the first region, the fuel jet turns entirely to droplets; this region is associated by Rayleigh–Taylor modeling; details and validation are available in [38].

The transport equations of the turbulent reacting flow are formulated as follow:

1. Species conservation equation Eq. (1):

$$\frac{\partial \overline{\rho}_k}{\partial t} + \nabla\left(\overline{\rho}_k \tilde{u}\right) = \nabla\left(\overline{\rho} D \, \Delta \bar{y}_k\right) + \nabla\phi + \overline{\rho}_k^c + \overline{\rho}_k^s \tag{1}$$

where $\bar{y}_k = \frac{\rho_k}{\rho}$ and $\varphi = \overline{\rho}_k \tilde{\boldsymbol{u}} - \overline{\rho_k \tilde{\boldsymbol{u}}}$.

2. Fluid continuity equation Eq. (2):

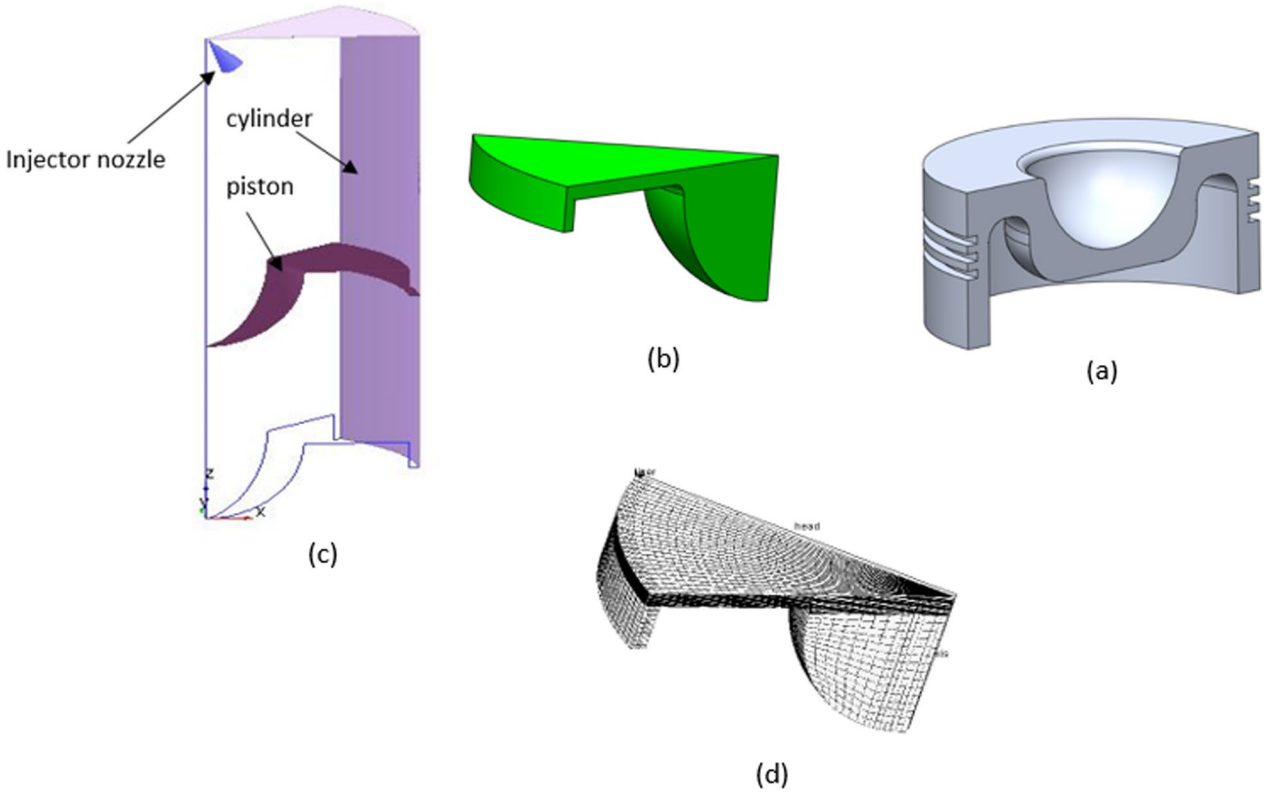

Fig. 2 geometry creating steps: **a** piston bowl, **b** computational sector, **c** piston sliding motion in the computational domain and **d** sector mesh

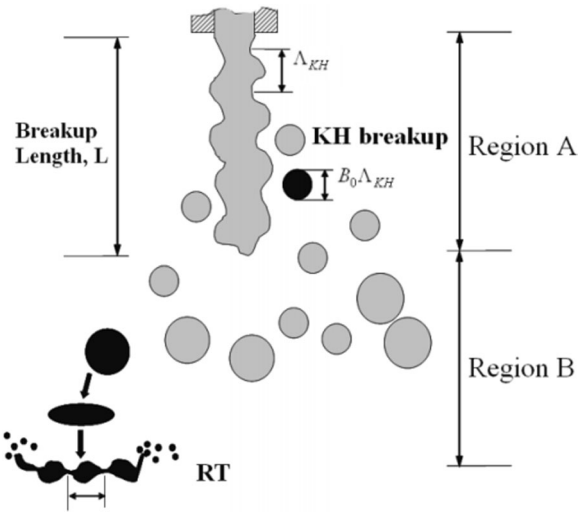

Fig. 3 KH/RT breakup model of fuel spray

$$\frac{\partial \overline{\rho}}{\partial t} + \nabla(\overline{\rho}\tilde{\boldsymbol{u}}) = \overline{\rho}^s \tag{2}$$

3. Momentum conservation equation Eq. (3):

$$\frac{\partial \overline{\rho}\tilde{\boldsymbol{u}}}{\partial t} + \nabla\left(\overline{\rho}\tilde{\boldsymbol{u}}\tilde{\boldsymbol{u}}\right) - \nabla\overline{P} + \nabla.\overline{\boldsymbol{\sigma}} - \Delta\Gamma + \overline{F}^s + \overline{\rho \boldsymbol{g}} \tag{3}$$

4. Energy conservation equation Eq. (4):

$$\frac{\partial \overline{\rho}\tilde{\boldsymbol{I}}}{\partial t} + \nabla\left(\overline{\rho}\tilde{\boldsymbol{u}}\tilde{\boldsymbol{I}}\right) = -\overline{P}\nabla\cdot\tilde{\boldsymbol{u}} - \nabla.\bar{J} - \nabla\mathbf{H} + \overline{\rho}\tilde{\varepsilon} + \overline{Q}^c + \overline{Q}^s \tag{4}$$

where $\bar{\boldsymbol{J}} = -\lambda\nabla\overline{T} - \overline{\rho}\,\mathrm{D}\sum\widetilde{\boldsymbol{h}_k}\nabla y_k$ and $\lambda = \overline{\rho}C_p\,\alpha$.

5. Gas-phase mixture equation of state Eq. (5):

$$\overline{P} = R_u\overline{T}\sum\frac{\overline{\rho_k}}{\overline{W_k}} \tag{5}$$

Turbulence is modeled by the renormalization group RNG k-ε [39] Eqs. (6,7).

$$\frac{\partial \overline{\rho}\widetilde{K}}{\partial t} + \Delta\left(\overline{\rho}\widetilde{u}\widetilde{K}\right) = -\frac{2}{3}\overline{\rho}K\widetilde{K}\nabla\cdot\widetilde{u} + (\sigma - \Gamma) : \nabla\cdot\widetilde{u} + \nabla\left[\frac{(\mu+\mu_T)}{\mathrm{Pr}_k}\nabla\widetilde{K}\right] - \overline{\rho}\widetilde{\varepsilon} + \overline{W}^s \tag{6}$$

Table 6 Values of RNG k-ε model constants

c_μ	0.085
$c_{\varepsilon 1}$	1.42
$c_{\varepsilon 2}$	1.68
$c_{\varepsilon 3}$	1.5
$1/Pr_k$	1.39
$1/Pr_\varepsilon$	1.39
η_0	4.38
B	0.012
C_s	1.5

Table 7 Boundary and initial conditions

Head temperature (K)	470
Liner temperature (K)	420
Piston temperature (K)	500
Initial pressure (bar)	1
Initial temperature (K)	370
Inflow droplet temperature (K)	320
Initial swirl ratio	1.5

$$\frac{\partial \overline{\rho}\tilde{\boldsymbol{\varepsilon}}}{\partial t} + \nabla \cdot (\overline{\rho}\tilde{\boldsymbol{u}}\tilde{\varepsilon}) = -\left(\frac{2}{3}C_{\varepsilon 1} - C_{\varepsilon 3}\right) \cdot \overline{\rho}\tilde{\varepsilon}\nabla \cdot \tilde{\boldsymbol{u}} + \nabla\left[\frac{(\upsilon + \upsilon_T)}{Pr_\varepsilon}\nabla\tilde{\varepsilon}\right] + \frac{\tilde{\varepsilon}}{\tilde{K}}C_{\varepsilon 1}(\overline{\boldsymbol{\sigma}} - \Gamma) \cdot \nabla\tilde{\boldsymbol{u}} - C_{\varepsilon 2}\overline{\rho}\tilde{\varepsilon} + C_s\overline{W}^s - \overline{\rho} \quad (7)$$

where $R = \frac{C_\mu \eta^3(1-\eta/\eta_0)}{1+\boldsymbol{\beta}\eta^3} \cdot \frac{\tilde{\varepsilon}^2}{\tilde{K}}$.

The values of model constants c_s, c_μ, $c_{\varepsilon 1}$, $c_{\varepsilon 2}$, $c_{\varepsilon 3}$, $1/Pr_k$, $1/Pr_\varepsilon$, η_0 and β are given in Table 6. Boundary and initial conditions are given in Table 7.

When the fuel droplets impinge the wall surface, this impingement will result in the following possibilities [40]:

1. Sticking if $We_n \leq 5$
2. Rebound if $5 < We_n \leq 10$
3. Spread if $We_n > 10$ and $We_n\, Re_n^{0.5} < H_{cr}$
4. Splash if $We_n\, Re_n^{0.5} \geq H_{cr}$

where $We_n = \frac{\rho U^2 d}{\sigma}$, $Re_n = \frac{\rho U d}{\mu}$ and $H_{cr} = [1500 + \frac{650}{\beta^{0.42}}][1 + 0.1Re_n^{0.5}\text{mim}(\delta, 0.5)]$.

Splash impingement regime is employed in the present work. The net heat release rate can be calculated by the first low Eq. (8).

$$\frac{dQ_{net}}{d\theta} = \frac{\gamma}{\gamma - 1}\,\mathrm{P}\,\frac{dV}{d\theta} + \frac{\gamma}{\gamma - 1}\,\mathrm{V}\frac{dP}{d\theta} \quad (8)$$

4.1 Model validation

Figures 4, 5 and 6 show a comparison of simulation and experimental results for in-cylinder pressure, heat release rate and in-cylinder temperature at 100% of engine rated load using diesel fuel. The experimental and computational results were found to be in agreement. The peak pressure deviation was approximately 2.7%. The heat release rate (HRR) plot had two peaks because combustion in a diesel engine occurs in two phases: premixed and diffusion. The rapid combustion (first peak in

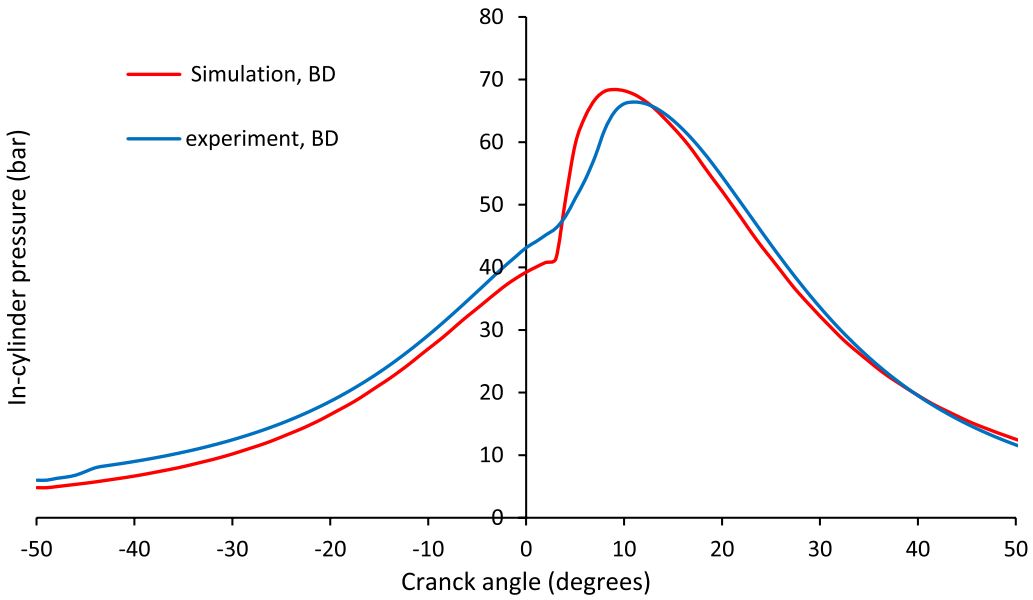

Fig. 4 In-cylinder pressure for the base diesel (BD) fuel at 100% of engine rated load

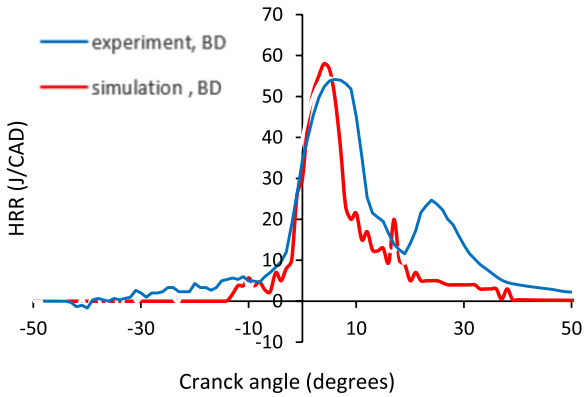

Fig. 5 Heat release rate (HRR) of base diesel fuel at 100% of engine load

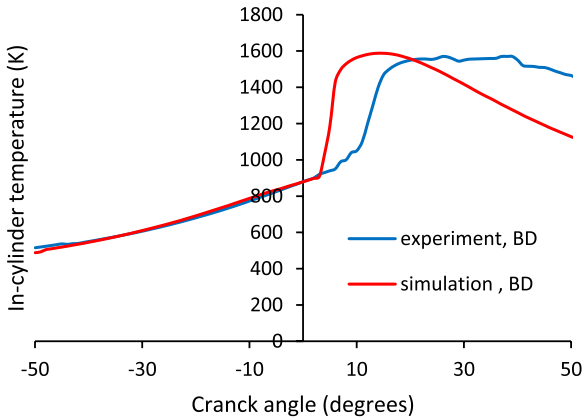

Fig. 6 In-cylinder temperature of base diesel fuel at 100% of engine load

Table 8 Comparison of numerical and experimental results of the BD fuel at 100% of engine rated load

Measured quantity	Numerical result	Experimental result	Difference (%)
Peak pressure (bar)	68.2	66.4	2.71
Peak temperature (K)	1593	1572	1.335
Peak HRR (J/deg)	57.4	54.5	5.32
BSFC (g/KWh)	311.4	303	2.77
BTE (%)	28.4	29.5	3.72
CO (g/Kg of fuel)	128.4	122.2	5.07
CO2 (g/Kg of fuel)	2691	2614.4	2.92
NO (g/Kg of fuel)	33.47	31.13	7.51
HC (g/Kg of fuel)	3.13	2.73	14.6
EGT (K)	696	711	2.1

Table 9 Rate of change in the results for biodiesel fuel compared to diesel fuel

Measured quantity (%)	Numerical result (%)	Experimental result [41]	Difference
BSFC	11.8	9	2.8
BTE	− 11.3	− 8.07	3.23
CO	− 42.38	− 46	3.62
CO2	11.2	5.63	5.57
NOx	21.8	17.62	4.18
HC	− 41.53	− 44	2.47
EGT	− 9.4	− 5.03	4.37

pressure and HRR plots) is due to the premixed combustion phase. Any changes in temperature, HRR (second peak) and pressure after the first phase inside the cylinder are due to the diffusion phase, and this phase can be controlled by mixing fuel with air. In this context, the first peak in the HRR plot is due to the premixed combustion phase, and its wider width indicates good mixing and the consumption of a large amount of fuel during this phase. The second peak size in the HRR plot indicates how much fuel was consumed during this phase. The experimental and simulation results do not match at the second peak in the HRR plot, as shown in Fig. 5. In addition, as shown in Fig. 6, a divergence was observed between the ends of the experimental and theoretical temperature lines. This indicates that combustion continued in the practical experiment, which could be because the injector continued to inject fuel even after combustion ended. As a result, in the practical experiment, a development occurred in the diffusion combustion phase that differed from the diffusion combustion in the numerical simulation. Table 8 compares the numerical and experimental performance and emission results for conventional diesel fuel at 100% engine rated load. A numerical simulation was conducted on the biodiesel fuel fired the diesel engine using a combination of methyl decanoate (MD), methyl-9-decanoate (MD9D) and n-heptane, where the MD represent the saturation FAME and the MD9D represent the unsaturation FAME, the validation and details of this mechanism are available in literature [35]. Table 9 compares the numerical results to the experimental results reported in the literature [41] (Additional file 1).

5 Results

5.1 Engine performance

Figures 7, 8 and 9 show the variation in mean pressure, heat release rate and temperature inside the engine cylinder at 100% of the engine rated load for biodiesel and base diesel fuel. As shown in Fig. 7, combustion of soybean biodiesel fuel begins earlier than combustion of base diesel fuel because the

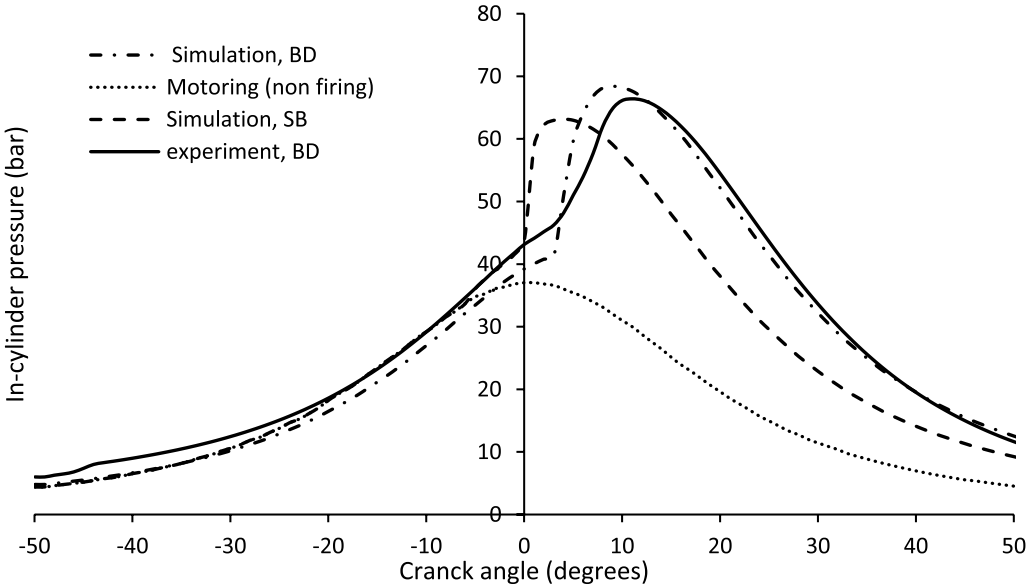

Fig. 7 In-cylinder pressure for base diesel (BD) and soybean biodiesel (SB) fuels at 100% of engine rated load

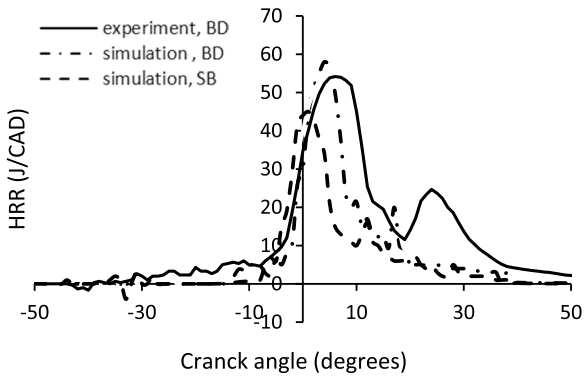

Fig. 8 Heat release rate (HRR) for base diesel (BD) and soybean biodiesel (SB) fuels at 100% of engine rated load

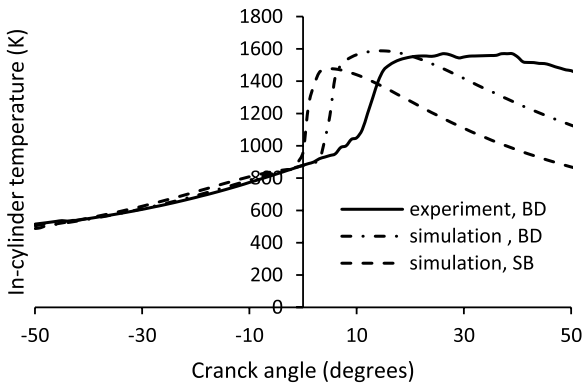

Fig. 9 In-cylinder temperature for base diesel (BD) and soybean biodiesel (SB) fuels at 100% of engine rated load

premixed phase of soybean biodiesel (SB) is shorter than that of base diesel (BD) or the biodiesel fuel has a shorter ignition delay period due to its higher cetane number. As a result, the in-cylinder pressure of the base diesel fuel increased because more fuel was injected during the premixed phase than in the soybean biodiesel fuel. Because of the lower heating value of soybean biodiesel fuel, the heat release rate HRR for biodiesel was reduced by an average of 21.8% at 100% of the engine rated load. These findings are consistent with those reported by [41, 42] (Additional file 2).

Figures 10 and 11 depict the variations in brake-specific fuel consumption (BSFC) and brake thermal efficiency (BTE) for base diesel and soybean biodiesel fuels at each load. The BSFC for soybean biodiesel fuel was found to be 11.8% higher than that of base diesel fuel, owing to the lower heating value of soybean biodiesel, which is about 12.8% lower than that of base diesel fuel. As a result, in order to produce the same power as diesel fuel, the amount of soybean biodiesel fuel injected into the combustion chamber must be increased. The conversion efficiency of the chemical energy content in a fuel into useful work is represented by the BTE. As shown in Fig. 11, the BTE increases as engine load increases, but the BTE for biodiesel fuel was found to be lower than base diesel fuel by an average value of 11.3%. This reduction is due to the lower ignition delay period and less area between firing and non-firing pressure curves.

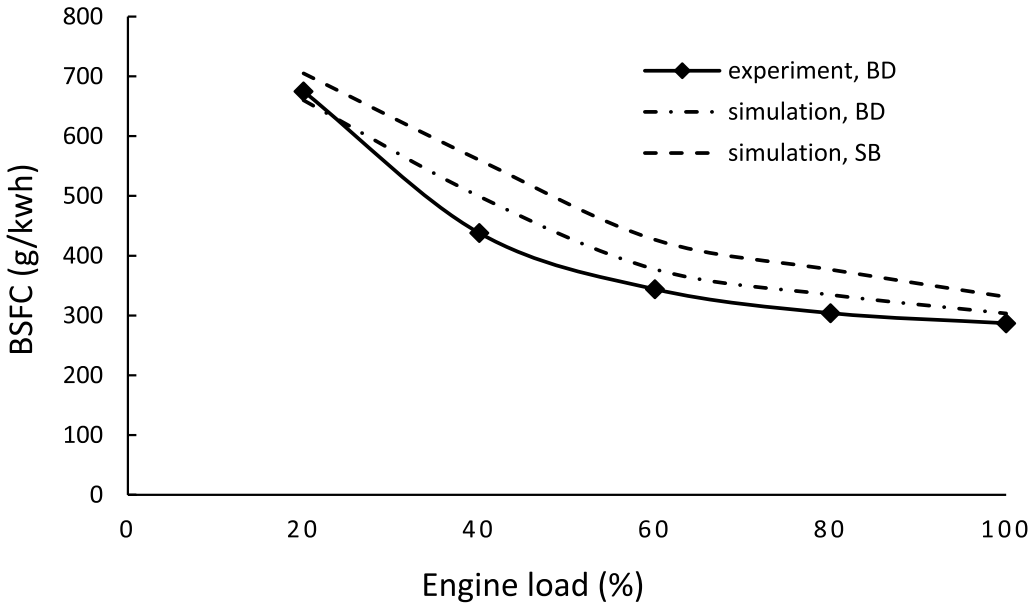

Fig. 10 Brake-specific fuel consumption (BSFC)

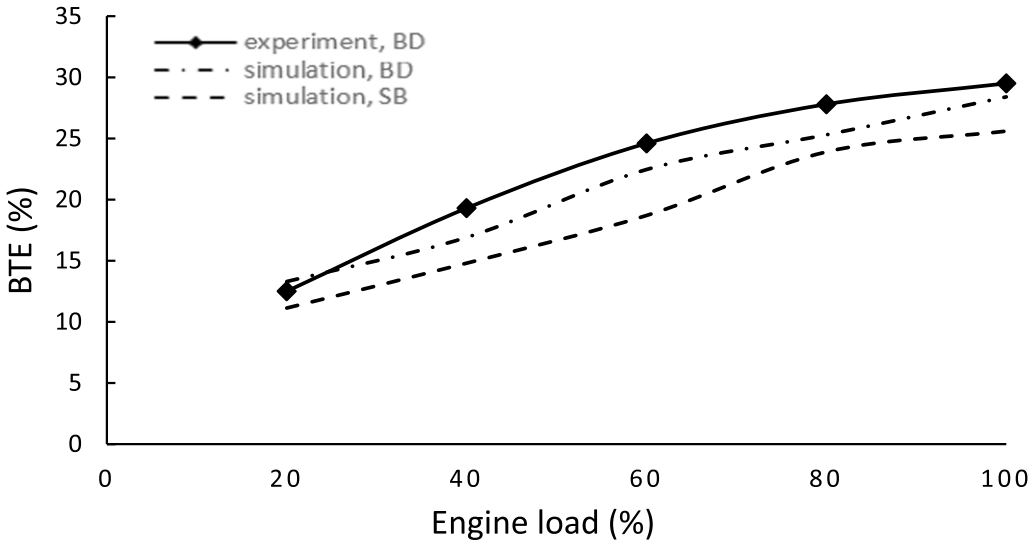

Fig. 11 Brake thermal efficiency (BTE)

5.2 Emission analysis

5.2.1 Carbon monoxide emission (CO)

Figure 12 depicts the CO emissions from the tested engine, which was powered by base diesel and soybean biodiesel fuels. It was found that increasing the engine load increases CO emissions for both diesel and soybean biodiesel fuels. At higher loads, CO emissions increase significantly due to a rich fuel mixture, which results in incomplete combustion. As illustrated in Fig. 12, soybean biodiesel fuel emits significantly lower CO emissions than diesel fuel over the entire engine load. The average reduction in CO emissions for soybean biodiesel fuel was approximately 42.389% when compared to base diesel fuel; this reduction is primarily due to the excess oxygen content, which improves combustion efficiency. According to Özener et al. [41] and Vellaiyan [42], biodiesel fuel reduces CO emissions by 46 and 33.8%, respectively.

5.2.2 Hydrocarbon (HC) emissions

The hydrocarbon (HC) emissions are produced when hydrocarbons such as CH_4 do not burn completely and exhausted out the engine. Figure 13 clearly shows that

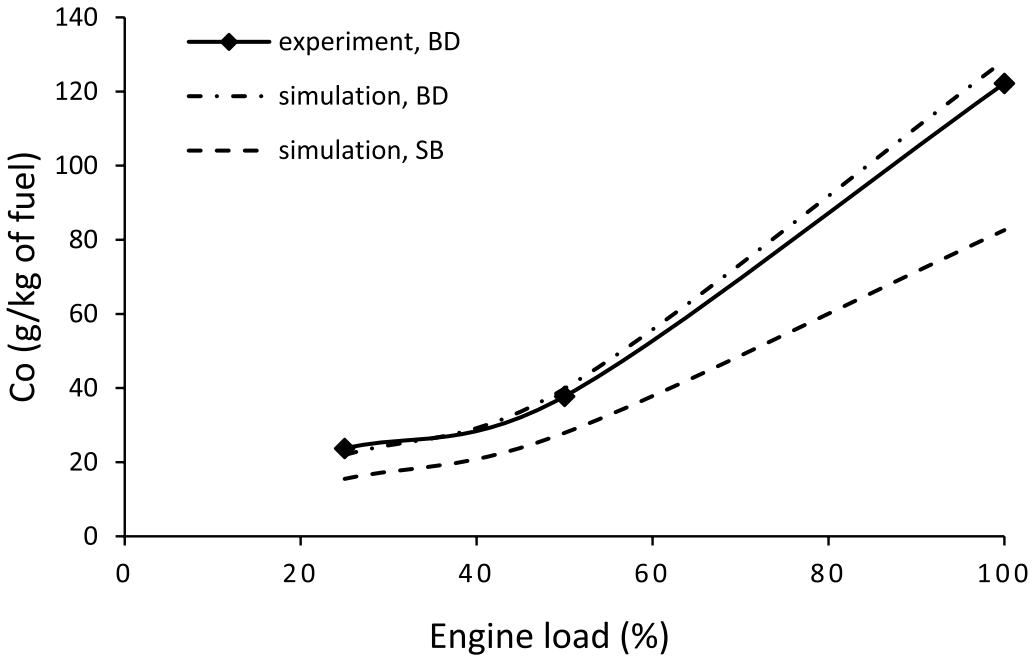

Fig. 12 CO emissions at different loads

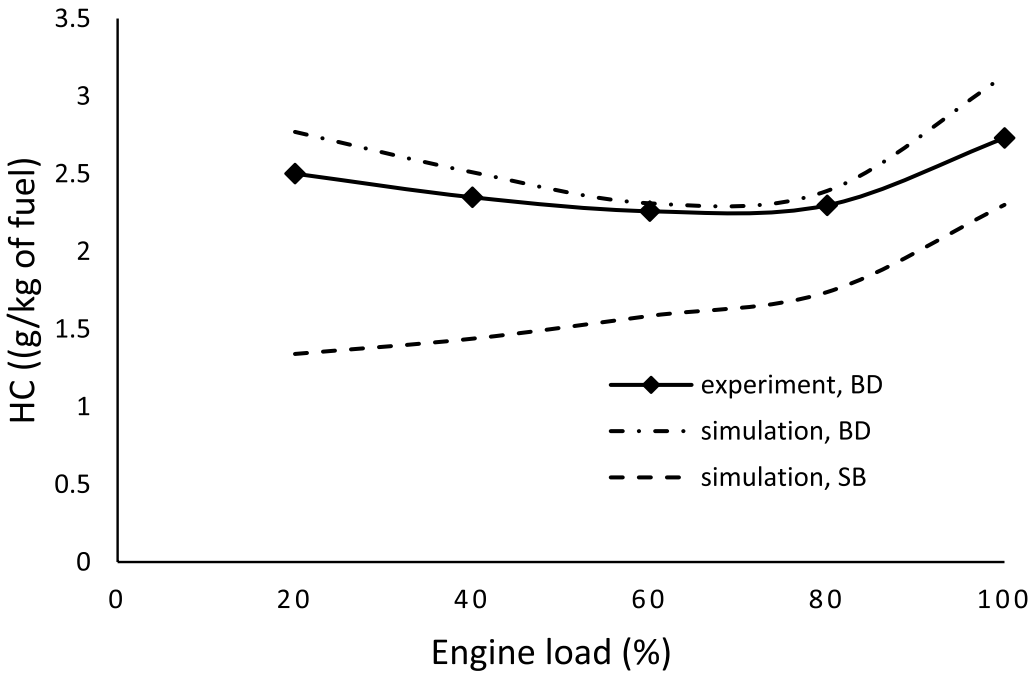

Fig. 13 HC emissions at different loads

the biodiesel fuel significantly reduces HC emissions compared to diesel fuel over the entire engine loads. On average, soybean biodiesel fuel reduces HC emissions by approximately 41.53% when compared to diesel fuel; this reduction is due to the higher cetane number and oxygen content of soybean biodiesel; this result is consistent with that reported by [42]. Furthermore, the higher the cetane number of biodiesel fuel, the shorter the ignition delay period, which influences the reduction of HC emissions.

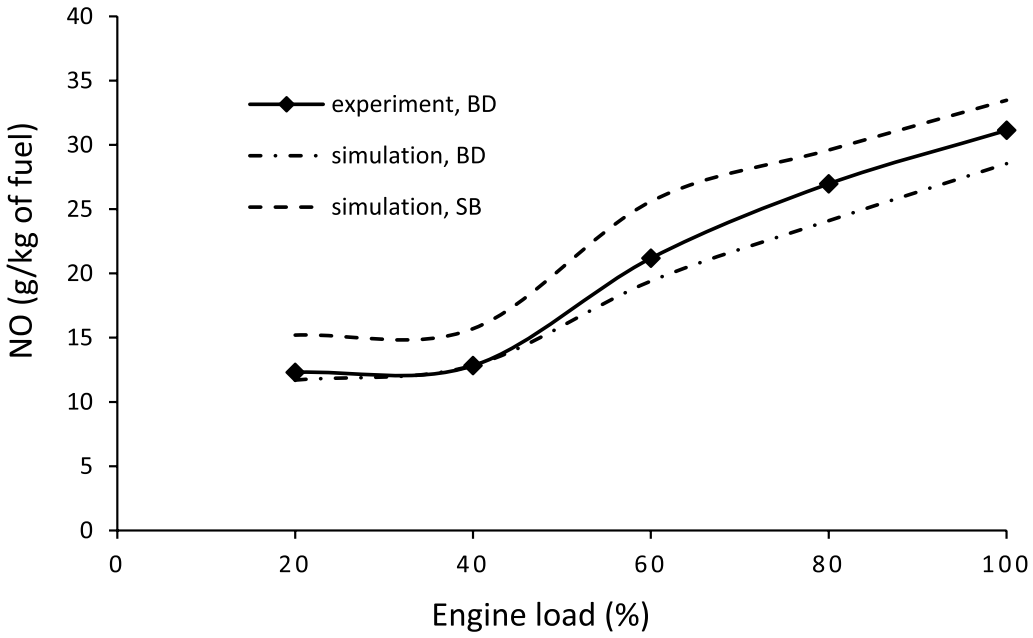

Fig. 14 NO emissions at different loads

5.2.3 Nitrogen oxide (NO_x) emissions

As shown in Fig. 14, nitric oxide (NO) emissions increase as engine load increases due to an increase in in-cylinder temperature, which results in the decomposition of more nitrogen atoms from atmospheric air, and these nitrogen atoms interact with oxygen to form the nitrogen oxides NO_x (NO and NO_2). In the combustion of soybean biodiesel fuel, the higher in some spatial temperature inside the engine cylinder, excess oxygen content and faster reaction rate are attained when compared to diesel fuel. As a result, NO_x formation in soybean biodiesel fuel is always greater than in diesel fuel. This study found that NO emissions increased by an average of 21.8% over the entire engine loads. The higher oxygen content of biodiesel is considered to be the main cause of higher NO_x emissions. As shown in Fig. 15, some zones in the combustion chamber reached higher temperatures than diesel fuel due to the unsaturated fatty acids present in soybean biodiesel fuels, resulting in more thermal NO_x formation. Because the intensity of the interaction of oxygen with carbon and nitrogen is greater in biodiesel fuel than in diesel fuel, regions with higher NO emissions have lower oxygen content.

5.2.4 Carbon dioxide (CO_2) emissions and exhaust gas temperature (EGT)

Because of the higher oxygen concentration and lower carbon-to-hydrogen ratio in biodiesel fuel, the fuel oxidation process occurs in locally rich zones during the combustion of biodiesel fuel in a diesel engine, reducing the tendency to produce soot. CO_2 emissions and EGT were calculated numerically for base diesel and soybean biodiesel fuels at different engine loads. As shown in Figs. 16 and 17, using biodiesel fuel increases Co_2 emissions and decreases EGT over the entire engine load range by an average of 11.2% and 9.4%, respectively. The lower EGT is due to the earlier combustion and the lower heating value of soybean biodiesel fuel.

5.3 Optimization

This study showed that the combustion of biodiesel fuel began earlier than diesel fuel with a drop in peak pressure so, optimization of the injection timing of biodiesel is essential.

Soybean biodiesel fuel is optimized by conduction four SOI timings as shown in Table 10. Figure 18 shows the in-cylinder combustion pressure of soybean biodiesel at wide range of SOI timings. In the case of SOI = − 15 bTDC, the combustion began earlier than diesel fuel by 1.44 CAD and the peak pressure was dropped by 4.37%, which mean that the in-cylinder peak pressure and temperature are increased and resulting in a higher engine performance compared to other SOI timings. The combustion characteristics of soybean biodiesel is optimum at SOI = − 15 bTDC.

6 Discussion

The combustion process in diesel engines is divided into two phases, as shown in Figs. 7 and 8. The first phase is the premixed phase, which begins after the start of

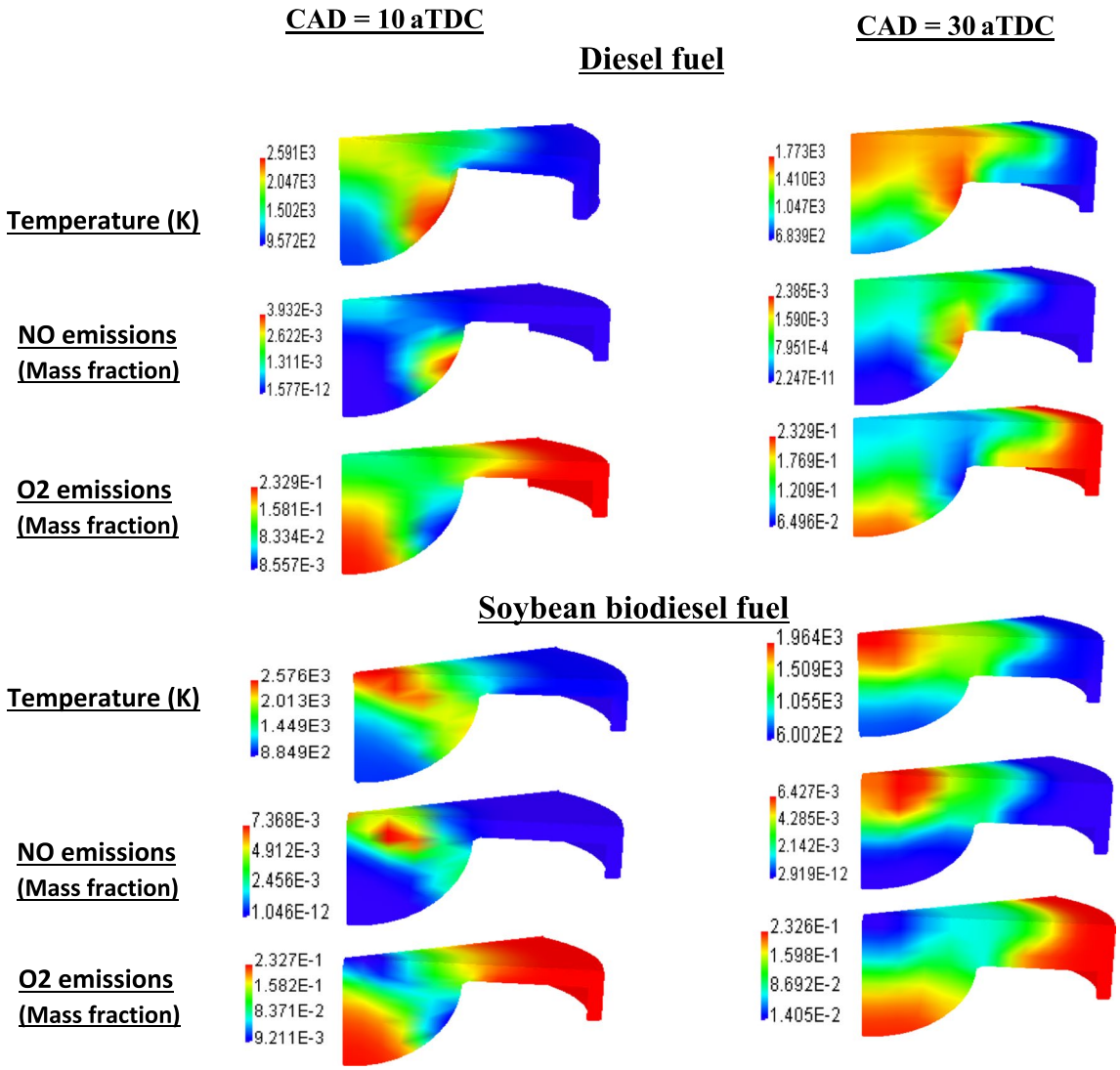

Fig. 15 Spatial distributed temperatures, NO and O_2 emissions at 10 CAD and 30 CAD aTDC for diesel and soybean biodiesel fuels

injection and involves the mixing of fuel and air to form combustible rich fuel zones. When a self-ignition occurs, multiple flames spread from various locations quickly consume all of the combustible mixture, causing pressure and temperature to rise rapidly and the combustion to transition to the second phase; diffusion phase. The premixed phase is responsible for the peak pressure and the first peak in the HRR diagram. The diffusion phase is governed by the mixing of air and fuel, which is responsible for any temperature change after the peak pressure, as illustrated in Fig. 9.

Diesel engine performance depends significantly on the fuel properties and the fuel injection system. Soybean biodiesel fuel is characterized by its higher viscosity, lower calorific value and the oxygenation nature so, these properties will affect fuel spray and combustion process. As shown in Fig. 7, the area between the firing and non-firing (motoring) pressure curves for the base diesel fuel is greater than that of soybean biodiesel fuel on the right-hand side, which this means the power delivered by the base diesel is higher than that of soybean biodiesel fuel.

Fuel spray is the process of forcing the liquid fuel out of a given container into a mass of small liquid droplets. In a DI diesel engine, the injector injects the fuel into the cylinder while it is still in the liquid phase. As soon as the injected liquid fuel enters the combustion chamber and comes into contact with the cylinder's air, the liquid phase instantly starts to disperse. This liquid phase evaporates, creating a combustible mixture that releases a considerable amount of energy inside the

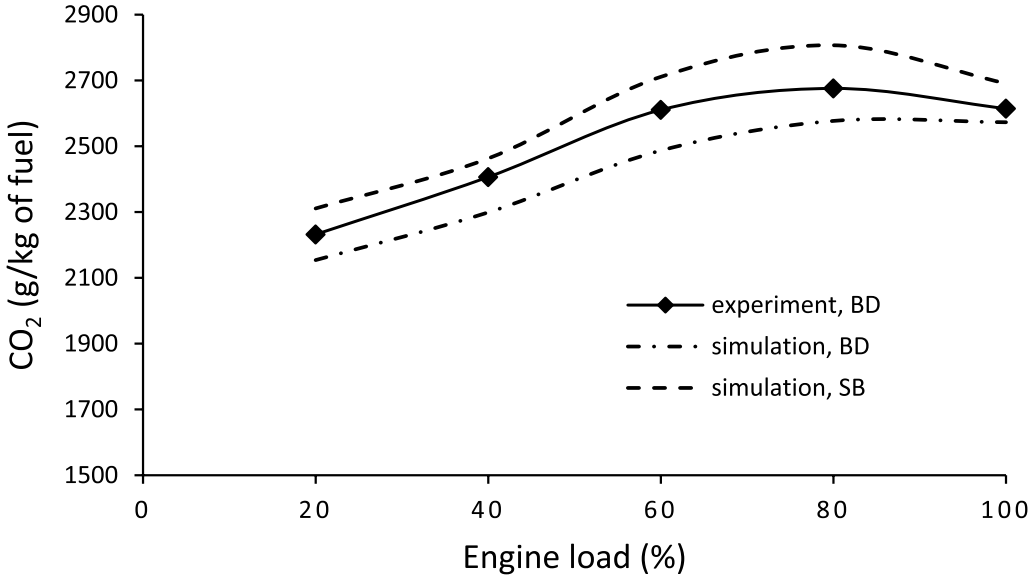

Fig. 16 CO_2 emissions at different loads

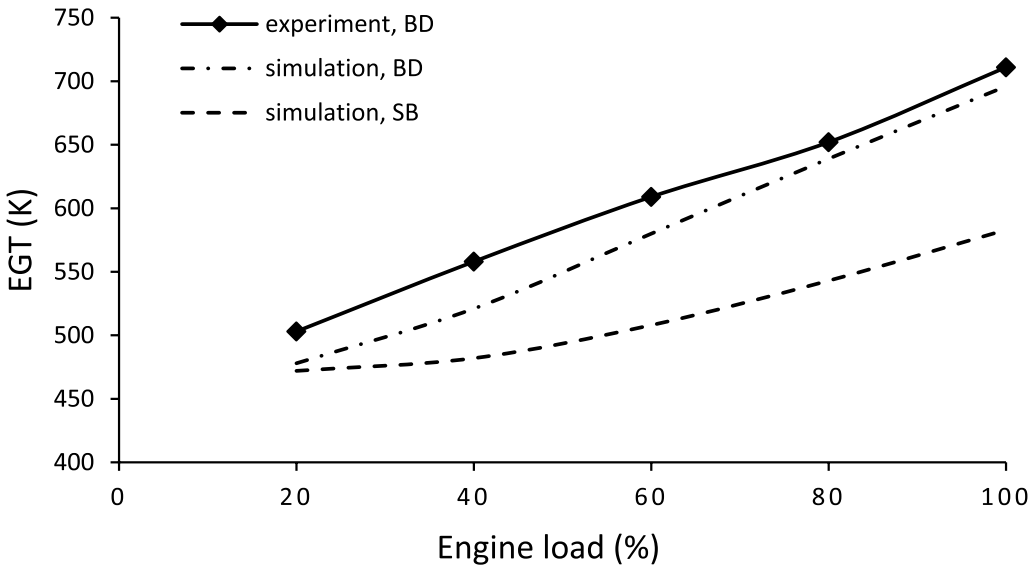

Fig. 17 Exhaust gas temperature (EGT) at different loads

Table 10 Start of injection timings of biodiesel fuel

SOI timing (bTDC)	Injection duration (CAD)
− 18	14.5
− 16	14.5
− 15	13.5
− 13.5	11.5

chamber. The entire process, which includes the atomization, evaporation and breakdown of the liquid fuel, is referred to as the spray evolution process. It is crucial to have a thorough understanding of spray evolution since it plays a significant role in the preparation of the mixture, which in turn affects how well the combustion and emission formation turn out. Using the particle-tracking tool in a CFD code, the spray behavior of the

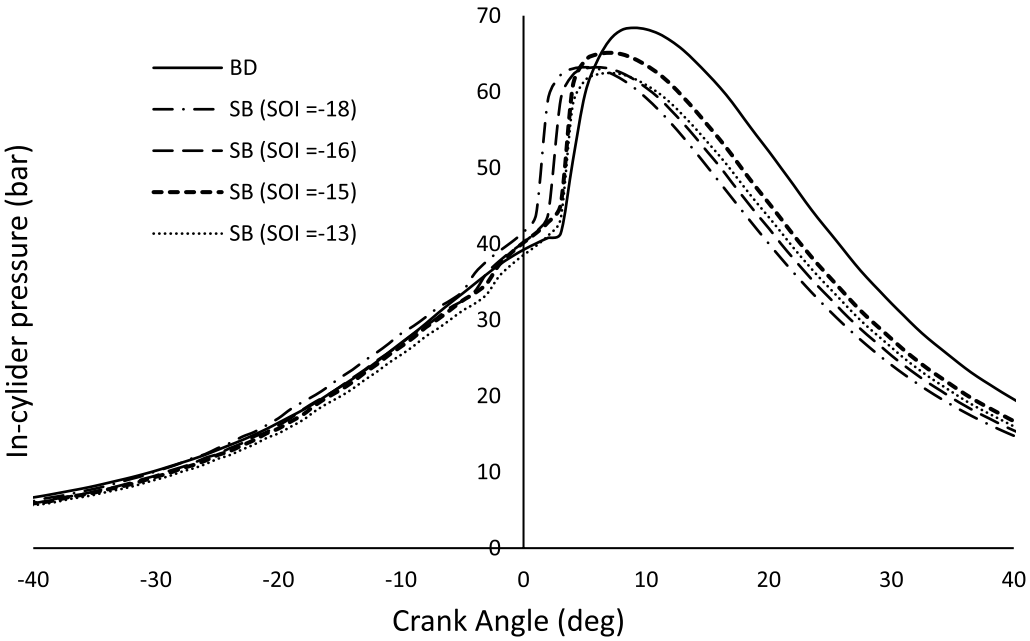

Fig. 18 In-cylinder pressure of soybean biodiesel at a wide range of SOI timings

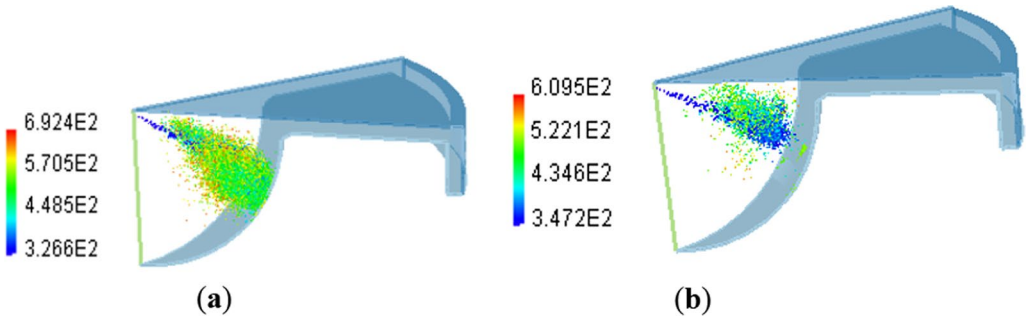

Fig. 19 Spray development of **a** diesel fuel and **b** biodiesel fuel

diesel and biodiesel fuels could be demonstrated in the current study in detail. The particle tracking of diesel and biodiesel sprays at TDC is shown in Fig. 19a and b. The two figures can be compared to demonstrate how much larger the spray cone angle of biodiesel is than that of diesel fuel and how much longer the liquid penetration length of biodiesel is than that of diesel. Additionally, the temperatures of diesel fuel droplets are higher than those of biodiesel fuel. These lower temperatures will have an impact on how well biodiesel evaporates, making it burn less efficiently than diesel.

Generally, the formation of carbon monoxide and hydrocarbon emissions is affected by fuel type, equivalence ratio, swirling, injection timing, engine load and engine speed. CO emission increases due to poor fuel atomization (low turbulence kinetic energy), rich fuel mixtures, high engine load and low speed (idle mode). The NOx formation is greatly influenced by the combustion temperature, oxygen concentration and reaction rate. The oxygen content in the biodiesel fuel is considered the main reason for the increase in NO_x emissions.

7 Conclusion

A 3-D computational fluid dynamics (CFD) study is carried out using a CFD code linked to a chemistry solver to analyze the performance and emission characteristics of a DI diesel engine fueled with base diesel (BD) and soybean biodiesel (SB) fuels. The diesel engine

was verified and a good validity was found. The following are the main findings of this study:

1) At different engine loads, the developed CFD model predicted in-cylinder pressure, temperature, heat release rate and CO, HC, CO2 and NOx emissions.
2) Because soybean biodiesel fuel has a lower ignition delay period than diesel fuel, the combustion process begins earlier, which is the main reason for lowering the area between the firing and non-firing (motoring) pressure curves for biodiesel fuel on the right-hand side, which increases the power delivered by the base diesel than that of soybean biodiesel fuel, so retarding biodiesel fuel injection to an angle near the TDC is preferred to overcome this deficiency.
3) In comparison with base diesel fuel, BSFC increased by an average of 11.8%, while BTE decreased by an average of 11.3% for soybean biodiesel fuel.
4) When compared to diesel fuel, the heat release rate of soybean biodiesel fuel was found to be about 21.8% lower at 100% of engine rated load.
5) When compared to diesel fuel, soybean biodiesel fuel reduced CO and HC emissions by an average of 42.38% and 41.53%, respectively.
6) Because the oxygen content in biodiesel fuel improved combustion efficiency and improved CO_2 conversion, NO_x and CO_2 emissions increased by 21.8% and 11.2%, respectively, when compared to diesel fuel.
7) The exhaust gas temperature (EGT) of soybean biodiesel fuel was reduced by 9.4% on average when compared to base diesel fuel.
8) Soybean biodiesel fuel was optimized by performing four starts of injection (SOI) at timings of − 18, − 16, − 15 and − 13,5 bTDC, and it was found that the combustion characteristics of soybean biodiesel are optimum at SOI = − 15 bTDC.

These findings indicate that biodiesel fuel can be used as an alternative and environmentally friendly fuel in the engine without requiring any modifications. Several strategies, such as exhaust gas recirculation (EGR) with fuel preheating and emulsion, can be used to address the problem of rising NO_x emissions.

Abbreviations

aTDC	After top dead center
bTDC	Before top dead center
BDC	Bottom dead center
BD	Base diesel
BSFC	Brake-specific fuel consumption (g/KWh)
BTE	Brake thermal efficiency
CAD	Crank angle degree
C_p	Heat capacity (J/K)
d	Droplet diameter (micron)
D	Diffusion coefficient
DI	Direct injection
EGT	Exhaust gas temperature (K)
FAMEs	Fatty acid methyl esters
$\overline{F}^s$	Momentum gain per unit volume due to the spray
g	Specific body force (ms-1)
h	Specific enthalpy (J/kgK)
H_{cr}	Splashing threshold
HRR	Heat release rate (J/CAD)
$\widetilde{I}$	Specific internal energy (J/kgK)
J	Heat flux vector (W/m.2)
K	Turbulent kinetic energy (m2s.−2)
k	Species index
P	Pressure (N/m.2)
$\overline{Q}^c$	Chemical heat release source term
$\overline{Q}^s$	Spray interactions source term
Re_n	Reynolds number
R_u	Universal gas constant (J/Kmol.K)
SB	Soybean biodiesel
SOI	Start of injection
TDC	Top dead center
$\overline{T}$	Fluid temperature (K)
v	Volume (m.3)
We_n	Weber number
$\overline{W}^s$	Eddies source term
W_k	Molecular weight (g/mol)
$\overline{y}_k$	Species mass fraction
σ	Specific body force (ms.−1)
β	Surface roughness height-to-incident droplet diameter ratio
γ	Specific heat ratio
δ	Film thickness-to-incident droplet diameter ratio
ε	Dissipation rate of the turbulent kinetic energy (m−2 s.−3)
θ	Crank angle
λ	Thermal conductivity (Wm−1 K.−1)
μ	Viscosity (N s m.−2)
υ_T	Turbulent kinematic viscosity (m2 s.−2)
ρ_	Density (kg/m.3)
ρ_k^c	Chemical reaction source term
ρ_k^s	Spray evaporation source term
σ	Viscous shear stress (N/m.2)
α	Thermal diffusivity (m2s.−1)

Supplementary Information

The online version contains supplementary material available at https://doi.org/10.1186/s43088-023-00349-w.

Additional file 1. Simulation of diesel engine combustion using soybean biodiesel fuel.

Additional file 2. Simulation of diesel engine combustion using base diesel fuel.

Acknowledgements
The authors would like to thank and acknowledge the support offered by the staff of internal combustion engines laboratory, faculty of engineering, Al-Azhar University, for their contributions to the experiments.

Author contributions
MKA conducted the numerical simulation, visualization, conceptualization and investigation and wrote the manuscript. MMA supervised the laboratory experiments and structured. AME conducted the laboratory experiments, edited, read and reviewed the final manuscript. All authors read and approved the final manuscript.

Funding
The authors declare that they did not receive any specific grant from funding agencies in the public, commercial or not-for-profit sectors.

Availability of data and materials
The data used in the present study are available on request.

Declarations

Ethics approval and consent to participate
Not applicable.

Consent for publication
Not applicable.

Competing interests
The authors declare that they have no competing interests.

Received: 29 November 2022 Accepted: 12 January 2023
Published online: 22 January 2023

References

1. Balasubramanian D, Lawrence KR (2019) Influence on the effect of titanium dioxide nanoparticles as an additive with Mimusops elengi methyl ester in a CI engine. Environ Sci Pollut Res 26:16493–16502. https://doi.org/10.1007/s11356-019-04826-7
2. Parthasarathy M, Ramkumar S, Isaac JoshuaRamesh Lalvani J, Elumalai PV, Dhinesh B, Krishnamoorthy R, Thiyagarajan S (2020) Performance analysis of HCCI engine powered by tamanu methyl ester with various inlet air temperature and exhaust gas recirculation ratios. Fuel 282:118833. https://doi.org/10.1016/j.fuel.2020.118833
3. Gao J, Tian G, Ma C, Balasubramanian D, Xing S, Jenner P (2020) Numerical investigations of combustion and emissions characteristics of a novel small scale opposed rotary piston engine fuelled with hydrogen at wide open throttle and stoichiometric conditions. Energy Convers Manage 221:113178. https://doi.org/10.1016/j.enconman.2020.113178
4. Ramalingam K, Balasubramanian D, Chellakumar PJTJS, Padmanaban J, Murugesan P, Xuan T (2020) An assessment on production and engine characterization of a novel environment-friendly fuel. Fuel 279:118558. https://doi.org/10.1016/j.fuel.2020.118558
5. Vellaiyan S (2020) Enhancement in combustion performance and emission characteristics of a biodiesel-fueled diesel engine by using water emulsion and nanoadditive. Renew Energy 145:2108–2120. https://doi.org/10.1016/j.renene.2019.07.140
6. Silitonga AS, Masjuki HH, Ong HC, Sebayang AH (2018) Evaluation of the engine performance and exhaust emissions of biodiesel-bioethanol-diesel blends using kernel-based extreme learning machine. Energy 159:1075–1087. https://doi.org/10.1016/j.energy.2018.06.202
7. Jin C, Zhang X, Geng Z, Pang X, Wang X, Ji J, Wang G, Liu H (2019) Effects of various co-solvents on the solubility between blends of soybean oil with either methanol or ethanol. Fuel 244:461–471. https://doi.org/10.1016/j.fuel.2019.01.187
8. Atmanlı A, Ileri E, Yüksel B (2015) Effects of higher ratios of n-butanol addition to diesel–vegetable oil blends on performance and exhaust emissions of a diesel engine. J Energy Inst 88:209–220. https://doi.org/10.1016/j.joei.2014.09.008
9. Telli GD, Altafini CR, Rosa JS, Costa CA (2018) Experimental analysis of a small engine operating on diesel–natural gas and soybean vegetable oil–natural gas. J Braz Soc Mech Sci Eng 40:1–10. https://doi.org/10.1007/s40430-018-1469-
10. Wei S, Wang F, Leng X, Liu X, Ji K (2013) Numerical analysis on the effect of swirl ratios on swirl chamber combustion system of DI diesel engines. Energy Convers Manage 75:184–190. https://doi.org/10.1016/j.enconman.2013.05.044
11. Su LW, Li XR, Zhang Z, Liu FS (2014) Numerical analysis on the combustion and emission characteristics of forced swirl combustion system for DI diesel engine. Energy Convers Manage 86:20–27. https://doi.org/10.1016/j.enconman.2014.05.023
12. Abdelrazek MK, Abdelaal MM, El-Nahas AM (2022) Piston bowl shape and biodiesel fuel effects on combustion and emission of diesel engines. J Eng Appl Sci 69:103. https://doi.org/10.1186/s44147-022-00158-5
13. Rabeti M, Jahanian O, Ranjbar A, Safieddin AS, Solmaz H (2023) Potential of semi-empirical heat transfer models in predicting the effects of equivalence ratio on low temperature reaction and high temperature reaction heat release of an HCCI engine. J Appl Comput Mech 9:45–57
14. Zhang Z, Lv J, Li W, Long J, Wang S, Tan D, Yin Z (2022) Performance and emission evaluation of a marine diesel engine fueled with natural gas ignited by biodiesel-diesel blended fuel. Energy 256:124662
15. EL-Seesy AI, He Z, Hassan H, Balasubramanian D. Improvement of combustion and emission characteristics of a diesel engine working with diesel/jojoba oil blends and butanol additive. Fuel. 2020;https://doi.org/10.1016/j.fuel.2020.118433
16. Zhang Z, Lv J, Xie G, Wang S, Ye Y, Huang G, Tan D (2022) Effect of assisted hydrogen on combustion and emission characteristics of a diesel engine fueled with biodiesel. Energy 254:124269. https://doi.org/10.1016/j.energy.2022.124269
17. Coughlin B, Hoxie A (2017) Combustion characteristics of ternary fuel Blends: pentanol, butanol and vegetable oil. Fuel 96:196–488. https://doi.org/10.1016/j.fuel.2017.01.104
18. Ng HK, Gan S, Ng JH, Pang KM (2013) Simulation of biodiesel combustion in a light -duty diesel engine using integrated compact biodiesel-diesel reaction mechanism. Appl Energy 102:1275–1287. https://doi.org/10.1016/j.apenergy.2012.06.059
19. Al-Dawody MF, Bhatti SK (2014) Experimental and computational investigations for combustion, performance and emission parameters of a diesel engine fueled with soybean biodiesel-diesel blends. Energy Procedia 52:421–430. https://doi.org/10.1016/j.egypro.2014.07.094
20. Ganesan N, Le TH, Ekambaram P, Balasubramanian D, Le VV, Hoang AT (2022) Experimental assessment on performance and combustion behaviors of reactivity-controlled compression ignition engine operated by n-pentanol and cottonseed biodiesel. J Clean Product 330:129781. https://doi.org/10.1016/j.jclepro.2021.129781
21. Nayak SK, Hoang AT, Nayak B, Mishra PC (2021) Influence of fish oil and waste cooking oil as post mixed binary biodiesel blends on performance improvement and emission reduction in diesel engine. Fuel 289:119948. https://doi.org/10.1016/j.fuel.2020.119948
22. Singh A, Sinha S, Choudhary AK, Sharma D, Panchal H, Sadasivuni KK (2021) An experimental investigation of emission performance of heterogenous catalyst Jatropha biodiesel using RSM. Case Stud Thermal Eng 25:100876. https://doi.org/10.1016/j.csite.2021.100876
23. Gritsenko A, Shepelev V, Fedoseev S, Bedych T (2022) Increase in the fuel efficiency of a diesel engine by disconnecting some of its cylinders. Facta Universitatis-Ser Mech Eng. https://doi.org/10.22190/FUME210914002G
24. Kodate SV, Yadav AK, Kumar GN (2020) Combustion, performance and emission analysis of preheated KOME biodiesel as an alternate fuel for a diesel engine. J Therm Anal Calorim 141:2335–2345. https://doi.org/10.1007/s10973-020-09814-5
25. Biswas S, Mukhopadhyay A (2022) Assessment of the quadruple injection strategy over triple injections to improve emissions, performance and noise of the automotive diesel engine. Facta Univ-Ser Mech Eng 20:321–339
26. Beutler T, Prchal N, Günthner M (2022) Numerical modeling of diesel and polyoxymethylene dimethyl ether spray in a high pressure chamber using the fischer primary breakup model. Automot Engine Technol 7:409–426. https://doi.org/10.1007/s41104-022-00120-w
27. Baek HM, Lee HM (2022) Spray behavior, combustion, and emission characteristics of jet propellant-5 and biodiesel fuels with multiple split injection strategies. Energies 15:2540. https://doi.org/10.3390/en15072540
28. Kuti OA, Sarathy SM, Nishida K (2020) Spray combustion simulation study of waste cooking oil biodiesel and diesel under direct injection diesel engine conditions. Fuel 267:11724. https://doi.org/10.1016/j.fuel.2020.117240
29. Hoang AT, Le AT (2019) Trilateral correlation of spray characteristics, combustion parameters, and deposit formation in the injector hole of a diesel engine running on preheated Jatropha oil and fossil diesel fuel. Biofuel Res J 6:909–919. https://doi.org/10.18331/BRJ2019.6.1.2.
30. Hoang AT, Tabatabaei M, Aghbashlo M, Carlucci AP, Ölçer AI, Le AT, Ghassemi A (2021) Rice bran oil-based biodiesel as a promising renewable fuel alternative to petrodiesel: a review. Renew Sustain Energy Rev 135:110204. https://doi.org/10.1016/j.rser.2020.110204

31. Rajamohan A, Gopal AH, Muralidharan KR, Huang Z, Paramasivam B, Ayyasamy T, Nguyen XP, Le AT, Hoang AT (2022) Evaluation of oxidation stability and engine behaviors operated by Prosopis juliflora biodiesel/diesel fuel blends with presence of synthetic antioxidant. Sustain Energy Technol Assess 52:102086. https://doi.org/10.1016/j.seta.2022.102086
32. Cankci M, Van Gerpen JH (2003) Comparison of engine performance and emissions for petroleum diesel fuel, yellow grease biodiesel, and soybean oil biodiesel. Trans ASAE 46:937–944. https://doi.org/10.13031/2013.13948
33. Pehan S, Jerman MS, Kegl M, Kegl B (2009) Biodiesel influence on tribology characteristics of a diesel engine. Fuel 88:970–979. https://doi.org/10.1016/j.fuel.2008.11.027
34. Alptekin E, Canakci M (2008) Determination of the density and the viscosities of biodiesel–diesel fuel blends. Renewable Energy 33:2623–2630. https://doi.org/10.1016/j.renene.2008.02.020
35. Jung JW, Lim YC, Suh HK (2020) A study on the mechanism reduction and evaluation of biodiesel with the change of mechanism reduction factors. Proc IMechE Part D: J Automobile Eng 234:3398–3413. https://doi.org/10.1177/0954407020931694
36. M. Raju, M. Wang, P.K. Senecal, S. Som, D. E. Longman (2012) A reduced diesel surrogate mechanism for compression ignition engine applications. Internal combustion engine division fall technical conference ICEF2012–9204. https://doi.org/10.1115/ICEF2012-92045
37. Hiroyasu H, Kadota T (1976) Models for combustion and formation of nitric oxide and soot in DI diesel engines. SAE Technical 85:513–526. https://doi.org/10.4271/760129
38. Beale JC, Reitz RD (1999) Modeling spray atomization with the Kelvin-Helmholtz / Rayleigh-T aylor hybrid model. Atom Sprays 9:623–650. https://doi.org/10.1615/AtomizSpr.v9.i6.40
39. Yakhot V, Orszag SA (1986) Renormalization group analysis of turbulence. I. basic theory. J Sci Comput 1:3–51. https://doi.org/10.1007/BF01061452
40. Han Z, Xu Z, Trigui N (2000) Spray/wall interaction models for multidimensional engine simulation. Int J Engine Res 146:1–127. https://doi.org/10.1243/1468087001545308
41. Özener O, Yüksek L, Ergenç AT, M.J.f. Özkan, (2014) Effects of soybean biodiesel on a DI diesel engine performance, emission and combustion characteristics. Fuel 115:875–883. https://doi.org/10.1016/j.fuel.2012.10.081
42. Vellaiyan S (2020) Combustion, performance and emission evaluation of a diesel engine fueled with soybean biodiesel and its water blends. Energy 201:117633. https://doi.org/10.1016/j.energy.2020.117633

Publisher's Note